RSC Advances

ROYAL SOCIETY OF CHEMISTRY

www.rsc.org/advances

Oxidative coupling of primary amines to imines under base-free and additive-free conditions over AuNPs/SBA-NH$_2$ nanocatalyst

Chinna Krishna Prasad Neeli, Saidulu Ganji, Venkata Siva Prasad Ganjala, Seetha Rama Rao Kamaraju and David Raju Burri*

Oxidative coupling of benzylamines to N-benzylbenzylimines under base-free and additive-free conditions is achieved over AuNPs/SBA-NH$_2$, which is one of the best catalysts due to its high activity, ease of separation and reusability apart from its facile preparation.

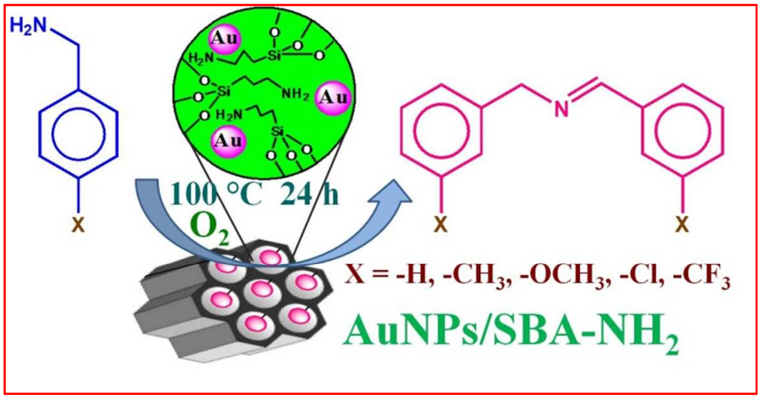

Cite this: DOI: 10.1039/c0xx00000x

www.rsc.org/xxxxxx

ARTICLE TYPE

Oxidative coupling of primary amines to imines under base-free and additive-free conditions over AuNPs/SBA-NH_2 catalyst

Chinna Krishna Prasad Neeli, Saidulu Ganji, Venkata Siva Prasad Ganjala, Seetha Rama Rao Kamaraju and David Raju Burri*

Received (in XXX, XXX) Xth XXXXXXXXX 20XX, Accepted Xth XXXXXXXXX 20XX
DOI: 10.1039/b000000x

4-12 nm sized AuNPs/SBA-NH_2 catalyst has been synthesized by post-synthetic functionalization of SBA-15 with propylamine followed by the deposition of Au^{3+} using $AuCl_3$ as a gold precursor and the reduction of Au^{3+} to metallic Au using $NaBH_4$ as a reducing agent. The structural and textural characteristics of AuNPs/SBA-NH_2 catalyst have been authenticated by XRD and N_2 adsorption techniques. FT-IR spectra validated the functionalized propylamine on the surface of SBA-15. The chemical state of gold species has been estimated by XPS and XRD techniques. The dispersion and particle size of Au species have been obtained from CO chemisorption. The particle size of Au species has also been determined by TEM analysis. The morphology of AuNPs/SBA-NH_2 catalyst has been determined from SEM technique. The AuNPs/SBA-NH_2 catalyst is capable of catalyzing the oxidative coupling of amines to imines effectively with a green O_2 oxidant at atmospheric pressure under base-free and additive-free conditions.

Introduction

Oxidation of amine to imine is an important chemical transformation, because the imines are highly versatile and ubiquitous synthetic intermediates for the synthesis of biologically active nitrogen containing compounds, fine chemicals and pharmaceuticals.[1] So far these industrially important oxidations are being carried out using stoichiometric oxidants such as 2-iodoxybenzoic acid,[2] or high valent inorganic reagents like chromate ions, permanganate ions, manganese dioxide and lead tetraacetate. [3] These processes inevitably lead to environmentally undesirable metal waste in large quantities. Traditionally, imines are being synthesized by the condensation of carbonyl compounds with amines in presence of Lewis acid catalysts e.g. $Ticl_4$.[4] However, these methodologies suffer from elevated temperatures, prolonged reaction times and requiring expensive dehydrating reagents.

Significant progress has been made in recent years in developing mild and practical methods for the synthesis of imines from condensation of amines with alcohols[5] and oxidation of secondary amines,[6] In contrast to the extensive work on secondary amines, little attention has been devoted to the oxidation of primary amines, which may be due to lower product selectivity.[7] Recently, direct catalytic oxidation of amines[8] to imines has been made utilize green oxidants[9,10] over transition metal catalysts such as ruthenium,[11] palladium,[12] copper,[13] TiO_2,[14] Nb_2O_5,[15] carbon nitride,[16] Fe^{3+} based MOFs,[17] microwave-assisted K-10 mont-morillonite system,[18] polyaniline-catalyzed[19] and manganese metalloporphyrins. [20]

Despite the gold catalysis is a prominent research area in recent years,[21-25]limited studies have been devoted for the synthesis of imines. With bulk gold catalysts the yield of imines are extremely low,[26] whereas with supported gold catalysts, particularly supported gold nanoparticle catalysts the yields of imines are in considerable amounts. [27-34] However, limited supported Au catalytic systems such as Au/γ-Al_2O_3, Au/C (activated carbon), Au/CeO_2, Au/TiO_2 etc., are reported for the oxidative coupling of amines to imines.

Among the family of mesoporous materials, SBA-15 silica is one of the most ideal catalyst supports due to its high surface area, high porosity, large and uniform pore size and potential applications.[35] These features provide a consistent and well isolated environment for the growth of nanoparticles, which is of particular interest for size dependent reactions. Despite the fact that SBA-15 is a robust and versatile support for various metal catalysts including gold, SBA-15 supported gold nanoparticles catalyst has not yet been investigated for the oxidative coupling of amines to imines. Furthermore, oxidative dehydrogenation of secondary amines to imines has considerably been investigated, whereas primary amines to imines have rarely been explored.

Herein, the synthesis of AuNPs/SBA-NH_2 solid catalyst and its characterization including its ability to catalyse the oxidative coupling of primary amines to corresponding imines with green O_2 oxidant at atmospheric pressure under base-free and additive-free conditions has been described.

Experimental

AuNPs/SBA-NH_2 heterogeneous catalyst has been prepared in three steps following the reported methods with slight modifications.[36]

Preparation of SBA-15

The siliceous SBA-15 was synthesized in accordance with the literature procedures and our previous publications [37]. All the reagents are obtained from commercial source and are used without further purification. In a typical synthesis, a solution of $EO_{20}PO_{70}EO_{20}$:2M HCl: TEOS: H_2O = 2:60:4.25:15 (mass ratio) was prepared using $EO_{20}PO_{70}EO_{20}$ (average $M_n \sim 5800$, Sigma-Aldrich, USA) as pluronic-P123 triblock copolymer and tetraethyl orthosilicate (TEOS, 98%, Sigma-Aldrich, USA) as silica source, stirred for 12 h at 40 °C and then hydrothermally treated at 100 °C under static condition for 24 h, subsequently filtered, dried the obtained solid mass at 100 °C and calcined at 550 °C for 8 h to remove the template. This template-free SBA-15 is used as a support in the preparation of desired AuNPs/SBA-NH_2 heterogeneous catalyst in subsequent steps.

Functionalization of SBA-15 with APTES (SBA-NH_2)

Prior to the functionalization, SBA-15 support was dried in an oven at 150 °C overnight under vacuum to remove physisorbed water. About 1 g of dried SBA-15 was dispersed in 60 ml of dry toluene, then 3 ml of 3-(Aminopropyl)triethoxysilane (APTES, 98%, Sigma-Aldrich, USA) was added and the mixture was refluxed for 24 h under anhydrous conditions according to our previous reports [38]. The solid product was recovered by filtration under vacuum, washed with 150 ml of toluene and dried at 100 °C in an air oven for 12 h, designated as SBA-NH_2.

Immobilization of AuNPs on SBA-NH_2

About 1 gm of SBA-NH_2 dispersed in 50 ml of ethanol (99.5%, Jiangsu Huaxi International Trade Co Ltd, China) solution containing 0.1714 mmol of $AuCl_3$ (99%, Sigma-Aldrich, USA) under N_2 atmosphere at room temperature followed by reduction with 0.1M sodium borohydride, $NaBH_4$ (98%, s d fine-chem Ltd, India) aqueous solution at room temperature for 12 h by adopting the reported procedure.[36, 39] The reddish brown mesoporous silica SBA-15 with embedded Au nanoparticles was washed with excess deionised water, filtered and dried at 100 °C under vacuum. This final catalyst was labelled as AuNPs/SBA-NH_2. For comparison Au/SBA-15 catalyst with larger Au particles was prepared using bare SBA-15 as a support.

Characterization of catalysts

The X-ray diffraction (XRD) patterns were recorded at room temperature using an X-ray diffractometer (Ultima-IV, M/s. Rigaku Corporation, Japan) with a nickel filtered CuKα radiation. N_2 adsorption–desorption isotherms were recorded on a N_2 adsorption unit at -196 °C (Quadrusorb-SI V 5.06, M/s. Quantachrome Instruments Corporation, USA). The samples were out-gassed at 200 °C for 4 h before the measurement. Infrared spectra were recorded on a (M/s. Perkin Elemer, Japan) FT-IR system, in the scan range of 4000–400 cm^{-1}. Au contents of the sample were analysed with a simutaneous ICP-AES allied analytical system (Perkin Elemer 3100XL). CO chemisorption measurements were carried out on AutoChem 2910 (Micromeritics USA) instrument. Transmission electron microscope (TEM) analysis was made using a Philips Technai G2 FEI F12 at an accelerating voltage of 80-100 kV. The SEM measurements with energy dispersive X-ray analysis (EDX) were performed on a JEOL 840A microscope operated at 10 kV accelerating voltage and 0.005 mA of beam current. The XPS analysis was made on a photoelectron spectrometer (KRATOS Axis 165, Shimadzu, Japan) with Mg Kα radiation (1253.6 eV).

Catalytic activity tests

The catalytic activity of AuNPs/SBA-NH_2 was tested in the oxidative coupling of benzylamine reaction. The catalyst was dried at 120 °C for 2 h before use. In a typical experiment, 0.4 mmol of substrate, 30 mg of AuNPs/SBA-NH_2 catalyst, 3 ml of toluene were taken in a RB flask and stirred magnetically at 100 °C under 1 atm O_2 pressure for 24 h, unless otherwise specified these conditions are applicable. The product mixture was analysed on a Gas Chromatograph (GC-17A Shimadzu) with WAX10 capillary column (30 m length × 0.53 mm internal diameter) and flame ionization detector. The products were confirmed by GC–MS (QP5050 model, M/s. Shimadzu Instruments, Japan) DB-5 column. (0.32 mm dia. and 25 m long, supplied by M/s. J & W Scientific, USA). The catalytic activity data is based on the calibrated GC/GC-MS analysis. Unless otherwise specified the yields are on the basis of GC/GC-MS.

$$\text{Conversion}(\%) = \frac{\text{nBA loaded} - \text{nBA consumed}}{\text{nBA loaded}} \times 100$$

$$\text{Selectivity}(\%) = \frac{\text{nNBBI produced}}{\text{nBA converted}} \times 100$$

$$\text{Yield}(\%) = \frac{\text{nNBBI produced}}{\text{nBA loaded}} \times 100$$

nBA = no. of moles of benzylamine, nNBBI = no. of N-benzylbenzylimine

Results and discussion

In the synthesized AuNPs/SBA-NH_2 catalyst the loading of propylamine is around 1.8 mmol/g (Table 1) and the loading of gold is approximately 2.01wt% (Table 1).

Table 1 Elemental analysis of SBA-15, SBA-NH_2 and ICP-AES result of AuNPs/SBA-NH_2 sample.

Sample	Analysis	C (%)	H (%)	N (%)	Au (%)
SBA-15	CHNS	NF	NF	NF	NF
SBA-NH_2	CHNS	8.91	2.40	2.52	-
AuNPs/SBA-NH_2	ICP-AES	-	-	-	2.01
AuNPs/SBA-NH_2	ICP-AES	-	-	-	1.98[a]

NF stands for not found. [a] Recycled catalyst after 4rd cycle

The structural and textural parameters of AuNPs/SBA-NH_2 catalysts were characterized by XRD and N_2 sorption techniques.

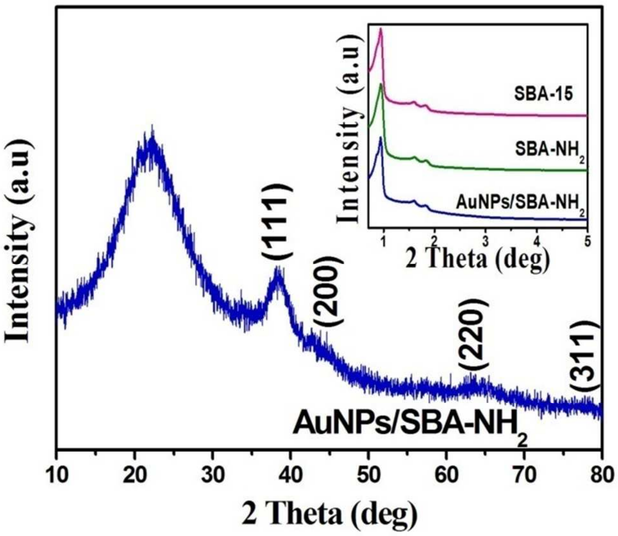

Fig.1 Wide-angle XRD pattern of AuNPs/SBA-NH$_2$ and low- angle XRD patterns (inset)

The wide-angle XRD pattern of AuNPs/SBA-NH$_2$ catalyst shown in Fig. 1 exhibits four diffraction peaks at 2θ = 38.1, 44.2, 64.7 and 77.5°, which correspond to (111), (200), (220) and (311) planes of fcc crystalline metallic Au in accordance with the JCPDS-ICDD 04-0784 and a broad peak that appears at 2θ ~ 22° is responsible for the SiO$_2$ phase of SBA-15[40]. Among the observed four diffraction peaks, the maximum intense peak corresponds to (111) plane, which is the predominant crystal facet. It is important note that the diffraction peaks of AuNPs/SBA-NH$_2$ catalyst are very broad and weak, suggesting the existence of low crystalline AuNps on the surface of SBA-15. The absence of large and intense diffraction peaks at higher angles confirms existence of Au particles [39] on SBA-15.

The Low- angle XRD patterns of SBA-15, SBA-NH$_2$, and AuNPs/SBA-NH$_2$ are also shown in Fig. 1(inset). Each pattern shows three well resolved peaks at 2θ = 0.95-1.1°, 1.63-1.7^o and 1.89-1.95^o respectively on the 2θ scale that are assigned to (100), (110) and (200) reflections, these results suggest that the two-dimensional hexagonal mesoporous structure of SBA-15[41] with space group *p6mm* remain intact at all the stages of AuNPs/SBA-NH$_2$ catalyst preparation.

The textural parameters of AuNPs/SBA-NH$_2$ catalysts were determined from N$_2$ sorption studies. The resultant N$_2$ adsorption-desorption isotherms of SBA-15, SBA-NH$_2$ and AuNPs/SBA-NH$_2$ are displayed in Fig. 2, where all the three isotherms are of type IV with H1 hysteresis loop and well defined step due to capillary condensation in the range 0.6–0.8 p/p$_0$, is the typical nature of ordered mesoporous materials with cylindrical pores in a narrow pore size distribution.[42] The results reveal that the retention of textural integrity at different stages of AuNPs/SBA-NH$_2$ catalyst preparation.

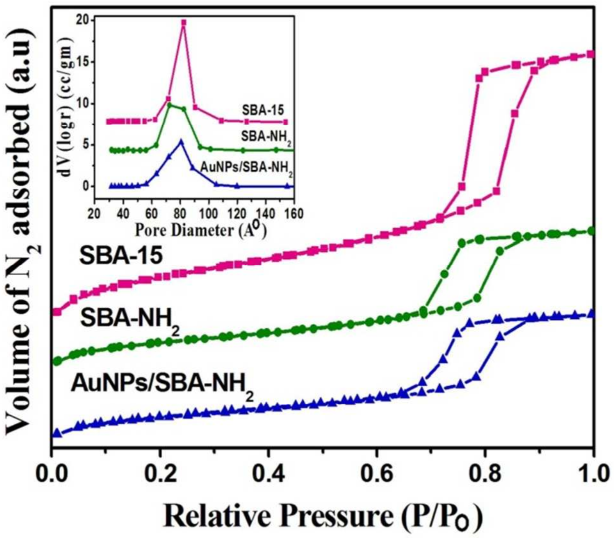

Fig.2 N$_2$ adsorption-desorption isotherms of SBA-15, SBA-NH$_2$ and AuNPs/SBA-NH$_2$ and pore size distribution curves (inset).

As shown Table 2, BET surface area, total pore volume and BJH pore diameter are in the decreasing order from SBA-15 to SBA-NH$_2$ and then to AuNPs/SBA-NH$_2$, which are due to partial blockage of certain pores by the functionalizing agent and Au nanoparticles. However, no substantial variation is observed in the structural parameters like d spacing and unit cell length, revealing the retention of SBA-15 structure both in SBA-NH$_2$ support and AuNPs/SBA-NH$_2$ catalyst.

Table 2 Textural and structural characteristics of SBA-15, SBA-NH$_2$ and AuNPs/SBA-NH$_2$ catalysts.

Catalyst	S_{BET}[a] (m^2/g)	V_t[b] (cc/g)	D_{BJH}[c] (nm)	d_{100}[d] (nm)	a_0[e] (nm)	t[f] (nm)
SBA-15	739	1.10	6.00	9.39	10.85	4.85
SBA-NH$_2$	435	0.81	5.52	9.27	10.71	5.19
AuNPs/SBA-NH$_2$	412	0.79	5.50	9.36	10.81	5.31

[a] BET surface area, [b] Total pore volume, [c] BJH$_{avg}$ pore diameter, [d] Periodicity of SBA-15 derived from low angle XRD, [e] Unit cell parameter (a_0=2 d_{100}/√3), [f] The pore wall thickness ($t=a_0-D_P$).

The FT-IR spectra of SBA-15, SBA-NH$_2$ and AuNPs/SBA-NH$_2$ are shown in Fig. 3. A broad band is observed in between 3437-3369 cm^{-1} in all the samples, which indicates typically –OH stretching vibration, the band at 1637 cm^{-1} is due to –OH deformation and the sharp band around 967 cm^{-1} is associated with Si-OH. The band at 3135 cm^{-1} in SBA-NH$_2$ is due to –NH$_2$ stretching vibration, which is in hydrogen bonding with –OH groups. New bands were observed in the range of 2932-2864 cm^{-1} and 1474-1384 cm^{-1} for SBA-NH$_2$ and AuNPs/SBA-NH$_2$, correspond to –CH$_2$ stretching and bending vibrations. The IR band at 1556 cm^{-1} corresponds to N–H (primary amine) bending vibrations. After propylamine functionalization, significant decrease in the intensities of absorption bands that are responsible for -OH groups in the stretching region (3437–3369 cm^{-1}) and

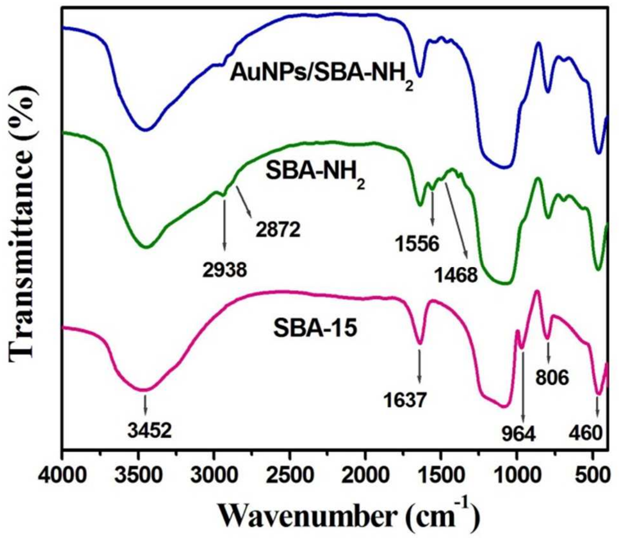

Fig.3 FT-IR spectra of SBA-15, SBA-NH$_2$ and AuNPs/SBA-NH$_2$

bending (967 cm^{-1}) regions, implies the consumption of –OH groups due to anchoring of propylamine onto SBA-15 through chemical bonding. For AuNPs/SBA-NH$_2$ an additional band at 1530-1560 cm^{-1} is observed which is due to –NH bending vibrations.[43] On the whole, IR spectra confirm the amine anchoring onto SBA-15.

TEM image (Fig.4) gives direct observation about the structural investigations of gold nanoparticles, which are highly dispersed inside the pore channels of functionalized SBA-15. The particle size distribution (PSD) bar graph reveals that most of AuNPs are in 4-12 nm size.

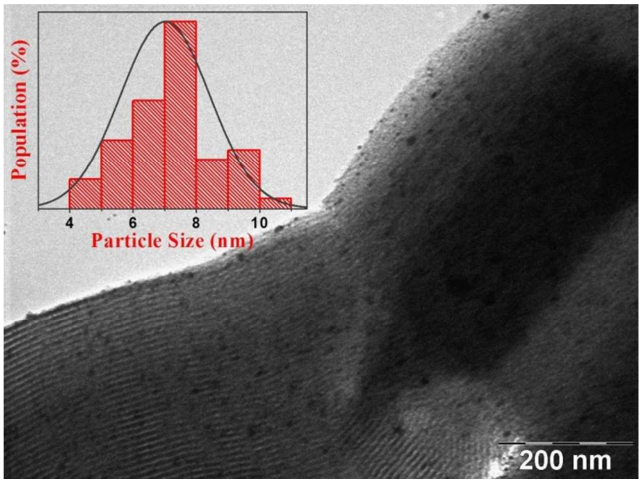

Fig.4 TEM image of AuNPs/SBA-NH$_2$ and PSD (inset).

The morphology of AuNPs/SBA-NH$_2$ catalyst was examined by SEM and the resultant image is shown in Fig.5a, which reveals cylindrical or wheat grain like morphology, commonly observed for siliceous SBA-15 materials. The energy dispersive X-ray (EDX) analysis was made and shown in Fig. 5b, confirms the immobilized Au nanoparticles on the surface of SBA-NH$_2$.

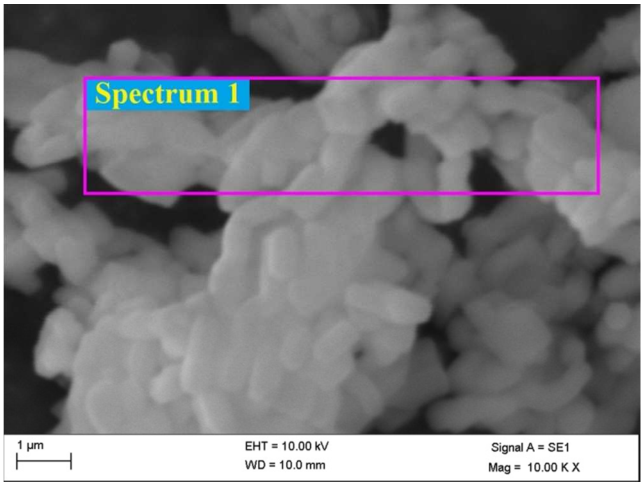

Fig.5a SEM image of AuNPs/SBA-NH$_2$ sample and rectangle represents the area of the EDX analysis (Fig. 5b)

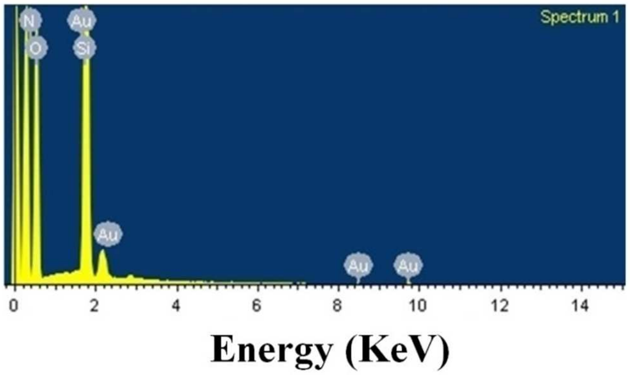

Fig.5b Typical energy dispersive X-ray analysis of Au nanoparticles on the surface of functionalised SBA-15.

Table 3 CO pulse chemisorption characteristics of supported Au catalysts

Catalyst	V_{CO}^{b} (ml/g)	S_{Au}^{c} (m^2/g)	P_{Au}^{d} (nm)	D_{Au}^{e} (%)
Au/SBA-15[a]	0.0794	12.06	22.75	4.50
AuNPs/SBA-NH$_2$	0.4227	49.14	06.32	18.48

[a] Au deposited on bare SBA-15 rather than SBA-NH$_2$, [b] Volume of CO uptake, [c] Au metal surface area, [d] Au particle size, [e] Au metal dispersion.

The physical properties of the catalysts such as metal dispersion, metal surface area and metal particle size obtained from CO pulse chemisorption technique (Table 3). The loading of Au is 2wt% in both Au/SBA-15 and AuNPs/SBA-NH$_2$ catalysts, but CO uptake, Au metal surface area and Au dispersion are greater than fourfold higher for AuNPs/SBA-NH$_2$ catalyst. Contrarily, the particle size of Au in AuNPs/SBA-NH$_2$ is very small. The results reveal that the functionalized propylamine groups may be restricting the mobility of gold particle, there by resisting the agglomeration of Au particles[44]. This phenomenon may be responsible for the higher dispersion of AuNPs on functionalized SBA-15.

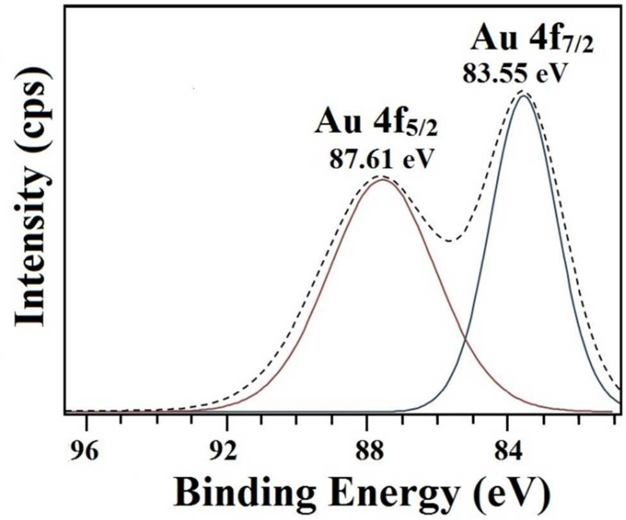

Fig.6 Au4f XPS spectrum of AuNPs/SBA-NH_2 sample.

As shown in Fig. 6, XPS spectrum exhibited doublet peak of zero valence Au4f$_{7/2}$ and Au4f$_{5/2}$ centered at about 83.55 and 87.61 eV, revealing metallic Au nanoparticles. When compared to standard binding energy values of metallic Au, 0.45 downshift of Au4f$_{7/2}$ and Au4f$_{5/2}$ from 84.0 eV and 88.0 eV, which may be due to strong metal interaction with functionalized propylamine groups which are in good agreement with the reported literature [45]. No cationic Au species is observed, confirming the complete reduction of $AuCl_3$ into metallic Au by $NaBH_4$ as reducing agent.

Among the imines synthesis processes, direct oxidative coupling of primary amines to imines is one of the important and eco-friendly processes. Hence, investigations are made over AuNPs/SBA-NH_2 catalyst choosing the oxidative coupling of benzylamine (BA) to *N-benzylbenzylimine* (NBBI) as a model reaction, where molecular oxygen has been used as an oxidant.

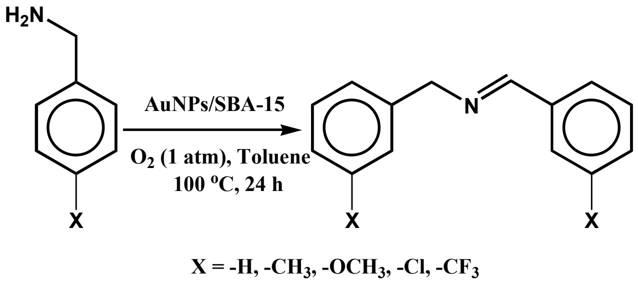

Scheme 1 Direct oxidative coupling of amines into imines.

Initially, the benzylamine was subjected to oxidative coupling using AuNPs/SBA-NH_2 (2.01%) as a heterogeneous catalyst and acetonitrile as a solvent at 80 °C for 24 h in O_2 (1atm). The conversion of benzylamine is 30% and the selectivity of *N-benzylbenzylimine* is 75%. When SBA-15 or SBA-NH_2 used as a catalyst, only a trace of *N-benzylbenzylimine* product was observed. When the reaction was conducted either in the N_2 atmosphere or in the absence of O_2 no detectable amount of *N-benzylbenzylimine* product was observed. It should be noted that the usage of a metal and O_2 or any other oxidant is obligatory for smooth running of oxidative coupling of benzylamine to *N-benzylbenzylimine* reaction. In the oxidative coupling of benzylamine over AuNPs/SBA-NH_2 catalyst, the main product is *N-benzylbenzylimine*. In brief, the molecular oxygen adsorbs on AuNps. The AuNPs activates the adsorbed O_2 while benzylamine molecule approaches. Reaction takes place between benzylamine molecule and the activated oxygen to form hydroperoxy (phenyl) methanamine intermediate, which on decomposition benzylimine produces through H_2O_2 elimination, which is a key intermediate in the reaction network [27](scheme 2). Through the alkylation of benzylimine with benzylamine by nucleophilic attack on the electron deficient imine carbon produces gem-diamine, which transforms into the desired *N-benzylbenzylimine* product by eliminating NH_3.[46] The Au-based catalysts partially dehydrogenate the primary amines into imine intermediate selectively rather than complete dehydrogenation to nitriles, [26] which is the unique property of Au-based catalyst compared to other popular dehydrogenation catalysts like ruthenium and copper.

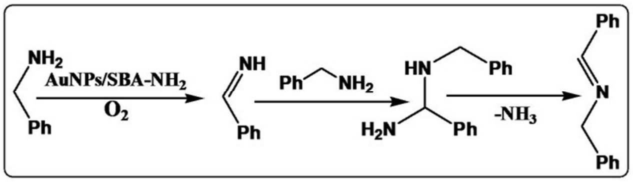

Scheme 2 Schematic representation of benzylamine oxidative coupling over AuNPs/SBA-NH_2 catalyst

With the intention to select the best solvent for oxidative coupling of primary amines to corresponding imines different solvents were tested at 80 °C and results are presented in Fig. 7, which reveals that there is a significant influence of solvents on the activity of AuNPs/SBA-NH_2 catalyst in benzylamine conversion and *N-benzylbenzylimine* selectivity. Both benzylamine conversion and *N-benzylbenzylimine* selectivity are more in toluene solvent compared to other solvents used. Hence, toluene is the best solvent for the oxidative coupling of benzylamine to *N-benzylbenzylimine* over AuNPs/SBA-NH_2 catalyst.

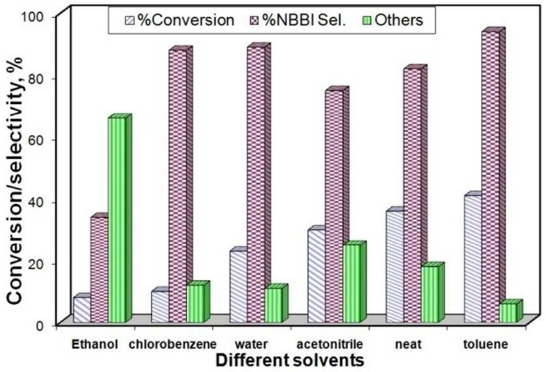

Fig.7 Effect of solvent on oxidative coupling of BA over AuNPs/SBA-NH_2 catalyst

To study the effect of reaction temperature on the oxidative coupling of benzylamine on AuNPs/SBA-NH_2 catalyst, different experiments were conducted at 80, 90 and 100 °C. At about 80 °C, the conversion of benzylamine was about 41%, which significantly increased to 76% when the reaction temperature was increased to 90 °C. With rise in reaction temperature from 80 to 90 °C, no significant changes were observed in the selectivity of *N-benzylbenzylimine*, which was more or less constant at 95%. When the reaction temperature was increased from 90 to 100 °C, the conversion reached to 92% with 98% selectivity of *N-benzylbenzylimine*. Since the boiling point of solvent (toluene) is close to 110 °C, further enhancement of reaction temperature is not feasible. Hence, the optimum reaction temperature is taken as 100 °C.

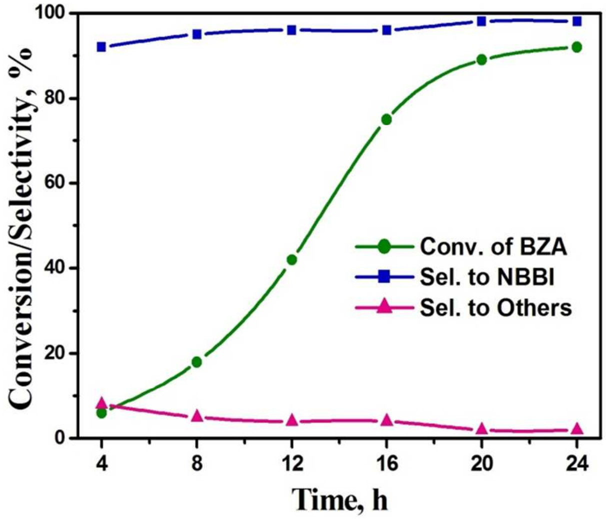

Fig. 8 Effect of reaction time on benzylamine oxidative coupling.

To understand the progress of the reaction with reaction time, six different experiments were conducted for 4, 8, 12, 16, 20 and 24 h keeping other reaction conditions constant and the results are displayed in Fig. 8. As the reaction time increases the conversion of benzylamine increased in a greater extent and attained maximum conversion of 92% with 98% selectivity of *N-benzylbenzylimine.* The selectivity of *N-benzylbenzylimine* is greater than 90% from 4 to 24 h experiments. The maximum yield of *N-benzylbenzylimine* is 90% in 24 h, which is taken as optimum reaction time.

Table 4 Scope of different substituted benzylamines in the oxidative coupling over AuNPs/SBA-NH_2 catalyst.

Entry	Substrate	Product	Yield [%]	TOF [h^{-1}]^a
1	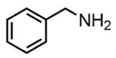	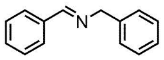	90	4.91
2	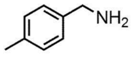	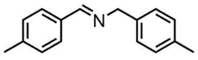	92	5.02
3	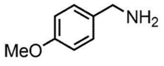	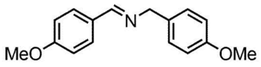	94	5.13
4	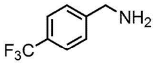	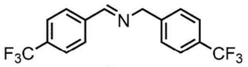	68	3.71
5	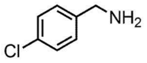	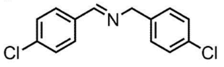	75	4.09

Conditions: Reactant (0.4 mmol); catalyst (30 mg, 0.76 mol% Au); O_2 (1 atm); Toluene (3 ml); Temperature (100°C); Time (24 h), GC-MS Yields.

[a] TOF is defined as the number of moles of product formed per moles of Au utilised per hour.

A variety of substituted benzylamines were subjected to oxidative coupling in the presence of O_2 over AuNPs/SBA-NH_2 solid catalyst and the results were displayed in Table 4. The reaction rates for benzylamines bearing electron-donating groups were significantly faster in comparison with electron-withdrawing variants (Table 4, entries 1–3). The p-methoxy benzylamine substrate achieved slightly faster reaction rate compared with p-chloro benzylamine (Table 4, entries 3 and 4). This is possibly due to a faster transamination for the phenylmethanimine intermediate when a more basic (electron-donating) amine is used. A noteworthy feature of our method is high TOF in the formation of imine product (Table 4, entry 1), which is a significant improvement over previously reported methods for the preparation of imines under atmospheric pressure.

The recyclability of the AuNPs/SBA-NH_2 catalyst was examined for the direct oxidative coupling of primary amines to corresponding imines under the optimized conditions (Figure 8).

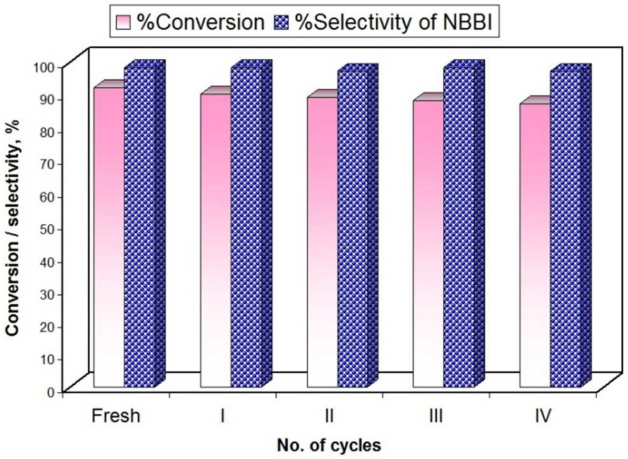

Fig.9 Reusability of AuNPs/SBA-NH_2 catalyst for oxidative dehydrogenation of benzylamine.

After the catalytic reaction, the catalyst was isolated from the liquid product by centrifugation, thoroughly washed with methanol, and then reutilized as catalyst in subsequent runs under identical reaction conditions. The results included in Fig. 8, indicating, no significant efficiency loss in 4 repeated cycles, revealing the stabilization of Au particles against leaching. The stabilization of AuNPs in the pore surfaces of SBA-NH_2 might have occurred through the interaction between the smaller holes that exists in the d-band of Au and lone pair electrons of functionalized amine nitrogen. Bond et al [47] reported that a small number of holes generates due to d-s hybridization in the d-band of Au during synthesis. The holes present in the d-band of Au may interact with the active π electrons of the functionalized vinyl groups on SBA-15, leading to good attachment and uniform distribution of gold nanoparticles.

The 92% conversion of benzylamine and 98% *N-benzylbenzylimine* at 100 °C in 24 h in the molecular oxygen, under additive-free and base-free conditions at atmospheric pressure is worth noting activity of AuNPs/SBA-NH_2 solid catalyst. The yield of *N-benzylbenzylimine* is 56% on bulk gold catalyst. Undoubtedly AuNPs/SBA-NH_2 is superior to bulk gold catalyst. Au/Al_2O_3 is one of the good heterogeneous catalysts, on which the yield of *N-benzylbenzylimine* is 92%, but the TOF is only 0.3 h^{-1}.[27] Au /CeO_2 is also one of the best catalysts, [31] yielded 89% of *N-benzylbenzylimine* with TOF of 3.2 h^{-1}. Among the reported best gold catalysts Au/C is the best catalyst, which produced 99% yield of *N-benzylbenzylimine*, unfortunately drastic deactivation is its demerit.[29] Au/TiO_2 is also a good catalyst with 92% yields, but operated at higher pressures (5 atm. O_2).[29] On the whole, AuNPs/SBA-NH_2 is one of the best catalysts due to its high activity, ease of separation and reusability apart from its facile preparation.

Conclusion

The AuNPs/SBA-NH_2 catalyst is highly active and selective towards the direct oxidative coupling of benzylamines to *N-benzylbenzylimines* under base-free and additive-free conditions with green O_2 oxidant at atmospheric pressure. The apparent high activity of the catalyst is ascertained from the nanoscale dispersion of AuNPs on diffusion-free hexagonally ordered mesoporous SBA-15 support containing propylamine moieties, which provides ease of AuNPs access to the reactant molecules and further more mesopores acts as nanoreactors for the reactant molecules.

Acknowledgements

Chinna Krishna Prasad and Saidulu are thankful to Council of Scientific and Industrial Research (CSIR) New Delhi, for awarding research fellowships.

References

1 S. I. Murahashi and Y. Imada, in *Transition Metals for Organic Synthesis, ed.* M. Beller and C. Bolm, 2nd edn, Wiley–VCH, Weinheim, Germany, 2004, vol. **2**, p. 497-507;

2 K. C. Nicolaou, C. J. N. Mathison and T. Montagnon, *Angew. Chem., Int. Ed.* 2003, **42**, 4077.

3 R. A. Sheldon and J. K. Kochi, *Metal Catalyzed Oxidations of Organic Compounds, Academic Press,* New York, 1981.

4 W. B. Jennings and C. J. Lovely, *Tetrahedron Lett.* 1988, **29**, 3725.

5 B. Gnanaprakasam, J. Zhang and D. Milstein, *Angew. Chem., Int. Ed.,* 2010, **49**, 1468.

6 T. Ishida, N. Kawakita, T. Akita and M. Haruta, *Gold Bull.,* 2009, **42**, 267.

7 K. Yamaguchi and N. Mizuno, *Angew. Chem.* 2003, **115**, 1518.

8 A. H. Ell, J. S. M. Samec, C. Brasse and J. E. Backvall, *Chem. Commun.,* 2002, 1144.

9 G. Chu and C. Li, *Org. Biomol. Chem.* 2010, **8**, 4716.

10 S. Kodama, J. Yoshida, A. Nomoto, Y. Ueta, S. Yano, M. Ueshima and A. Ogawa, *Tetrahedron Lett.,* 2010, **51**, 2450.

11 A. Prades, E. Peris and M. Albrecht, *Organometallics,* 2011, **30**, 1162.

12 J. R. Wang, Y. Fu, B. B. Zhang, X. Cui, L. Liu and Q. Xi. Guo, *Tetrahedron Lett.,* 2006, **47**, 8293.

13 R. D. Patil and S. Adimurthy, *RSC Advances,* 2012, **2**, 5119.

14 X. Lang, H. Ji, C. Chen, W. Ma and J. Zhao, *Angew. Chem. Int. Ed.,* 2011, **50**, 3934.

15 S. Furukawa, Y. Ohno, T. Shishido, K.Teramura and T. Tanaka, *ACS Catal.,* 2011, **1**, 1150.

16 F. Su, S. C. Mathew, L. Mohlmann, M. Antonietti, X. Wang and S. Blechert, *Angew. Chem., Int. Ed.,* 2011, **50**, 657.

17 A. Dhakshinamoorthy, M. Alvaro, and H. Garcia, *ChemCatChem,* 2010, **2**, 1438.

18 S. M. Landge, V. Atanassova, M. Thimmaiah and B. Torok, *Tetrahedron Lett.,* 2007, **48**, 5161.

19 K. Chi, H. Y. Hwang, J. Y. Park and C. W. Lee, *Synth. Met.,* 2009, **159**, 26.

20 Q. L. Yuan, X. T. Zhou and H. B. Ji, *Catal. Commun.,* 2010, **12**, 202.

21 G. C. Bond, P. A. Sermon, G. Webb, D. A. Buchanan and P. B. Wells, *J. Chem. Soc. Chem. Commun.* 1973, 444.

22 M. Haruta, T. Kobayashi, H. Sano and N. Yamada, *Chem. Lett.* 1987, **2**, 405.

23 M. Haruta, N. Yamada, T. Kobayashi and S. Ijima, *J. Catal.,* 1989, **115**, 301.

24 G. J. Hutchings, *J. Catal.* 1985, **96**, 292.

25 C. Della Pina, E. Falletta, L. Prati and M. Rossi, *Chem. Soc. Rev.,* 2008, **37**, 2077.

26 B. Zhu and R. J. Angelici, Chem. Commun., 2007, 2157.

27 B. Zhu, M. Lazar, B. G. Trewyn and R. J. Angelici, *J. Catal.,* 2008, **260**,1.

28 M. H. So, Y. Liu, C. M. Ho and C. M. Che, *Chem. Asian J.,* 2009, **4**, 1551.

29 A. Grirrane, A. Corma and H. Garcia, *J. Catal.,* 2009, **264**, 138.

30 S. Kegnaes, J. Mielby, U. V. Mentzel, C. H. Christensen and A. Riisager, *Green Chem.,* 2010, **12**, 1437.

31 L. Aschwanden, T. Mallat, F. Krumeich and A. Baiker, *J. Mol. Catal. A: Chem.,* 2009, **309**, 57.

32 L. Aschwanden, B. Panella, P. Rossbach, B. Keller and A. Baiker, *ChemCatChem,* 2009, **1**, 111.

33 H. Sun, F. Z. Su, J. Ni, Y. Cao, H. Y. He and K. N. Fan, *Angew. Chem., Int. Ed.,* 2009, **48**, 4390.

34 H. Guo, M. Kemell, A. Al-Hunaiti, S. Rautiainen, M. Leskela and T. Repo, *Catal. Commun.,* 2011, **12**, 1260.

35 H. X. Li, F. Zhang, Y. Wan and Y. F. Lu, *J.* Phys. Chem. B, 2006, **110**, 22942.

36 X. Liu, A. Wang, X. Wang, C-Y Mou and T. Zhang *Chem. Commun.,* 2008, 3187.

37 (a) D. Zhao, J. Feng, Q. Huo, N. Melosh, G. H. Fredrickson, B.F. Chmelka and G.D. Stucky, *Science*, 1998, **279**, 548 (b) A. Narani, K. H. P. Reddy, S. Vinukonda, K. S. Rama Rao and D. R. Burri, *Micropor.Mesopor. Mater.,* 2011, **143,** 132 (c) S. Ganji, B. Padma, V. Venkateswarlu, K. S. Rama Rao and D. R. Burri, *Catal. Sci. Technol*., 2013, **3**, 409 (d) C. K. P. Neeli, A. Narani R. K. Marella, K. S. Rama Rao and D. R. Burri *Catal. Commun.,* 2013, **39**, 5.

38 (a) A. Narani, R. K. Marella, R. Pochamoni, K. S. Rama Rao and D. R. Burri, *RSC Adv.,* 2014, **4**, 3774 (b) S. Ganji, S. Mutyala, C. K. P. Neeli, K. S. Rama Rao and D. R. Burri, *RSC Adv.,*2013, **3**,11533.

39 K. K. R. Datta, B. V. Subba Reddy, Katsuhiko Ariga and Ajayan Vinu, *Angew. Chem. Int. Ed.* 2010, **49**, 5961.

40 G.R. Rao and B.G. Mishra, *Mater. Chem. Phys.* 2005, **89**, 110.

41 D. Zhao, Q. Huo, J. Feng, B. F. Chmelka and G. D. Stucky, *J. Am.Chem. Soc.,* 1998, **120**, 6024.

42 K. S. W. Sing, D. H. Everett, R. A. W. Haul, L. Moscou, R. A. Pierotti, J. Rouque ' rol and T. Siemieniewska, *Pure Appl. Chem.,* 1985, **57**, 603.

43 Sujandi, S.-E. Park, D.-S. Han, S.-C. Han, M.-J. Jin and T. Ohsuna, *Chem. Commun.*, 2006, 4131.

44 Y. S. Chi, H. P. Lin and C. Y. Mou, *Appl. Catal. A. Gen.,*2005, **284,** 199.

45 L. Wang, X. Meng, B. Wang, W. Chi and F. S. Xiao, *Chem. Commun.,* 2010, **46**, 5003.

46 B. Zhu, M. Lazar, B. G. Trewyn, R. J. Angelici, *J. Catal*. 2008, **260** **(1)**, 1.

47 C. L. G, C. Bond, T. D. Tompson, Catalysis by Gold, Imperial College Press, London, 2006 (b) P. Wu, P. Bai, K. P. Loh and X.S. Zhao, *Catal. Today*, 2010, **158**, 220

Catalysis Laboratory, Indian Institute of Chemical Technology, Hyderabad-500607, INDIA. Fax: +91-40-27160921; Tel: +91-40-27191712; E-mail: david@iict.res.in